GA–A24873

ADVANCES IN COMPREHENSIVE GYROKINETIC SIMULATIONS OF TRANSPORT IN TOKAMAKS

by
R.E. WALTZ, J. CANDY, F.L. HINTON, C. ESTRADA-MILA, and J.E. KINSEY

OCTOBER 2004

DISCLAIMER

GA–A24873

ADVANCES IN COMPREHENSIVE GYROKINETIC SIMULATIONS OF TRANSPORT IN TOKAMAKS

by
R.E. WALTZ, J. CANDY, F.L. HINTON, C. ESTRADA-MILA,* and J.E. KINSEY†

This is a preprint of a paper to be presented at the 20th IAEA Fusion Energy Conference, Vilamoura, Portugal, November 1–6, 2004 and to be published in the *Proceedings.*

*University of California, San Diego, California, USA.
†Lehigh University, Bethlehem, Pennsylvania, USA.

Work supported by
the U.S. Department of Energy
under DE-FG03-95ER54309 and DE-FG02-92ER54141

GENERAL ATOMICS PROJECT 03726
OCTOBER 2004

Advances in Comprehensive Gyrokinetic Simulations of Transport in Tokamaks

R.E. Waltz,[1] J. Candy,[1] F.L. Hinton,[1] C. Estrada-Mila,[2] and J.E. Kinsey[3]

[1]General Atomics, P.O. Box 85608, San Diego, California 92186-5608, USA
[2]University of California, San Diego, California, USA
[3]Lehigh University, Bethlehem, Pennsylvania, USA

e-mail contact of main author: waltz@fusion.gat.com

Abstract. A continuum global gyrokinetic code GYRO has been developed to comprehensively simulate core turbulent transport in actual experimental profiles and enable direct quantitative comparisons to the experimental transport flows. GYRO not only treats the now standard ion temperature gradient (ITG) mode turbulence, but also treats trapped and passing electrons with collisions and finite β, equilibrium ExB shear stabilization, and all in real tokamak geometry. Most importantly the code operates at finite relative gyroradius (ρ_*) so as to treat the profile shear stabilization and nonlocal effects which can break gyroBohm scaling. The code operates in either a cyclic flux-tube limit (which allows only gyroBohm scaling) or globally with physical profile variation. Bohm scaling of DIII-D L-mode has been simulated with power flows matching experiment within error bars on the ion temperature gradient. Mechanisms for broken gyroBohm scaling, neoclassical ion flows embedded in turbulence, turbulent dynamos and profile corrugations, are illustrated.

1. Introduction

This paper exemplifies recent advances in gyrokinetic simulations of tokamak transport and notes future challenges. GYRO development began in 1999 and reached its major design milestones in early 2003 [1]. It is presently the most advanced gyrokinetic code. GYRO is a physically comprehensive nonlinear continuum (Eulerian) gyrokinetic code which can treat either (i) gyroBohm scaled flux tubes at vanishing ρ_* or (ii) full-radius and full-torus core profiles at small but finite ρ_* ($\rho_* = \rho_s/a$ where $\rho_s = c_s/\Omega_i$ is the ion sound gyroradius). It contains the physics needed for physically realistic simulations of the tokamak core: toroidal ITG physics, trapped and passing electrons, electron-ion pitch angle collisions, electromagnetic effects up to the ideal beta limit, real geometry, ExB and magnetic flutter transport. These features are in common with the similar predecessor flux tube continuum gyrokinetic code GS2 [2] and the more recent PIC flux tube code GEM [3] against which GYRO has been successfully benchmarked. GYRO operating in a nearly full radius slice at finite ρ_* uniquely has both ExB and diamagnetic rotational shear stabilization which can effectively break gyroBohm scaling [4], as well as parallel rotational shear drive. We refer to simulations with these features has having the "full physics" needed for quantitative agreement with experiments. During the past year we have added neoclassical flows and drivers with conservative Krook ion-ion collisions, multiple ion species for impurity and plasma pinch studies, and feedback methods for simulations at fixed flows rather than the conventional fixed gradients. The latter is the first step to a future steady state gyrokinetic transport code. The versatility of GYRO with either artificial or experimental profile input, and with either flux-tube or global operation, allows many applications, some of which we review here.

2. Formulation of the Global Continuum Gyrokinetic Code GYRO

GYRO solves the standard electromagnetic nonlinear gyrokinetic (and Poisson-Ampere) equations [5] for fluctuations about a given profile of shifted Maxwellian distributions. An Eulerian (continuum) rather than Lagrangian (PIC) discretization is used [1]. Recently, we have used a 2nd order implicit-explicit Runge-Kutta scheme [6] which treats the electron parallel advection implicitly, removing the stiff term in the gyrokinetic-Maxwell system and allowing faster runs. This also improves stability over purely explicit methods and allows larger radial slices in electromagnetic simulations, since the implicit advance moves the n=0

Poisson-Ampere field inversion farther from the long wavelength singularity which is troublesome with radial slices of more than a few hundred ion gyrolengths. Real tokamak geometry is treated with local MHD equilibria (as formulated by Miller [7,8]) about nested flux surfaces labeled by the midplane minor radius r (normalized to the outer minor radius a). GYRO uses a sparce grid but grid convergence (resolution) is always checked. Simulations of a radial slices with profiles have "benign" zero value boundary conditions, i.e. do not affect the slice interior [4]. An adaptive source[4] is used to maintain given driving gradients.

It is important to say that the 5-D gyrokinetic GYRO does not retain all the physics of the 6-D collisional Vlasov or Maxwell-Boltzmann system. All the terms in the gyrokinetic equation [5] are explicitly first order in ρ_*. In particular gyroBohm scaling is broken only by the effect of the profile variation. There are no explicitly next order ρ_* terms like the so-called parallel nonlinearity. Various small ρ_* approximations are made for numerical tractability and consistency. For example: the next order terms in the ballooning mode eikonal derivative and nonlinear terms in the Poisson-Ampere equations are dropped. Such next order terms break exact gyroBohm scaling even without profile variation and may well be important in the pedestal region where $\rho_s/L_{T,n}$ and $\tilde{n}/n_0$ could be 10% instead of 1% characteristic of the core. First order gyrokinetic equation may not apply with good accuracy in the pedestal. We believe accuracy can only be determined by comparison to a 6-D Vlasov simulation.

3. Full Physics Simulations of Bohm-scaled DIII-D L-mode Dimensionally Similar ρ_* Pairs

Since the first 1990 DIII-D ρ_* scaling experiments [9], it has been difficult to understand how gyroBohm-*sized* transport can have Bohm *scaling* at such very small ρ_* values; and furthermore why Bohm scaling is experimentally associated only with the ion channel in L-modes. A good quantitative understanding of the mechanisms breaking gyroBohm scaling still eludes us. Our primary focus [10] has been on obtaining physically comprehensive simulations of the Bohm-scaled DIII-D L-mode dimensionally similar pairs [11], understanding what physical mechanisms are required to get the Bohm scaling, as well as finding a quantitative match of the simulated and experimental power flows. Figure 1 shows the radial profile of the effective (combined channel) energy diffusivity $\chi_{eff} \equiv (\chi_i + \chi_e)/2$ normed to the gyroBohm unit diffusivity $\chi_{GB} \equiv (c_s/a)\rho_s^2$ at the norming radius r/a=0.6 for $\rho_* = 0.0026$ (2.1 T DIII-D discharge 101391) and $\rho_* = 0.004$ (1.05 T DIII-D discharge 101381). The parameters of this matched pair at the norm point are $r/a = 0.6$, $R/a = 2.68$, $a/L_{Ti} = 2.88$, $a/L_{Te} = 3.13$, $a/L_n = 1.35$, $T_i/T_e = 0.89$, $q = 1.50$, $\hat{s} = dlnq/dr = 1.02$, elongation $\kappa = 1.5$, and triangularity $\delta = 0.05$. The collisionality is $\nu_{ei}/[c_s/a] = 0.174$ and $\beta = 1.1\%$ (about 1/3 critical). Apparently the diffusivity at the norm point is not strongly dependent on 3-fold variation in the radial slice size suggesting that nonlocal effects are minimal here. When the diffusivities are normed to gyroBohm, the larger ρ_* discharge will have the smaller normed diffusivity by the ratio of the ρ_* values, i.e. 0.004/0.0026 = 1.53 compared to 9/6. The experimental values at the norm point are considerably lower at 2.1/1.3 = 1.6 but close to the Bohm scaling ratio $\left(\chi_B \equiv \chi_{GB}/\rho_*\right)$. The collisional exchange between ion and electron channels prevents meaningful separation but the simulated ion energy flows are about 2 times larger than the electron flows. Figure 1 simulations used heavier electrons $\sqrt{m_i/m_e} = 20$ instead of 60 for deuterium to speed-up the code for larger boxes.

Figure 2(a) shows small slice runs with the correct ratio $\sqrt{m_i/m_e} = 60$. Even though the heavier electrons overestimate the correct maximum growth rate $\gamma_{max} = 0.3\,[c_s/a]$ (at r/a = 0.60 by only 10%, the corrected mass ratio drops the transport levels by 2-fold yet still maintain the Bohm ratio. This is apparently due to the competition between γ_{max} and the ExB shear stabilization rate $\gamma_E = (r/q)\partial(q/r)V_E/\partial r = 0.13[c_s/a]$ (at r/a = 0.6) which can quench the turbulence entirely. Here $\gamma_E/\gamma_{max} \approx 0.5$ is less than a quench value of 1 ± 0.3 suggested by circular ITG gyrofluid studies [12] although similar studies in real geometry indicate $\gamma_E/\gamma_{max} \approx 0.5$ can quench the turbulence [8]. In fact it is also shown that turning off the experimental equilibrium sheared ExB profile again doubles the energy transport but the

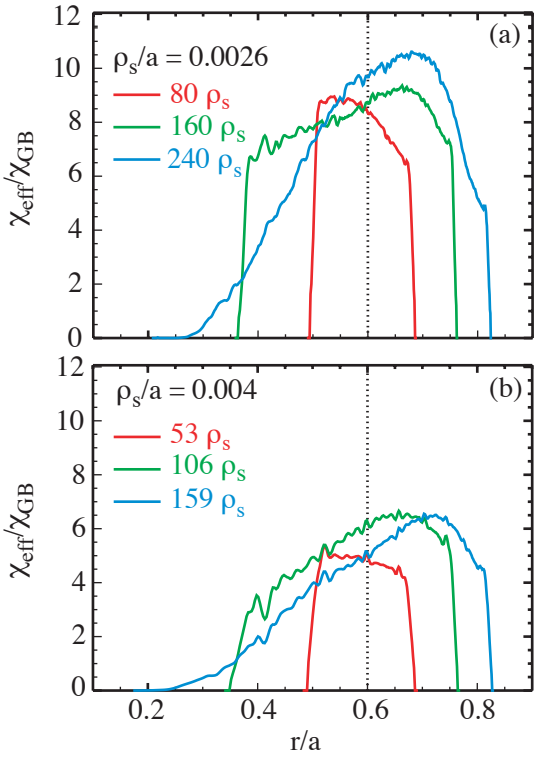

Fig. 1. Effective one channel energy diffusivity normed to gyroBohm at r/a=0.6 $\rho_* = 0.0026$ in (a) and $\rho_* = 0.004$ in (b).

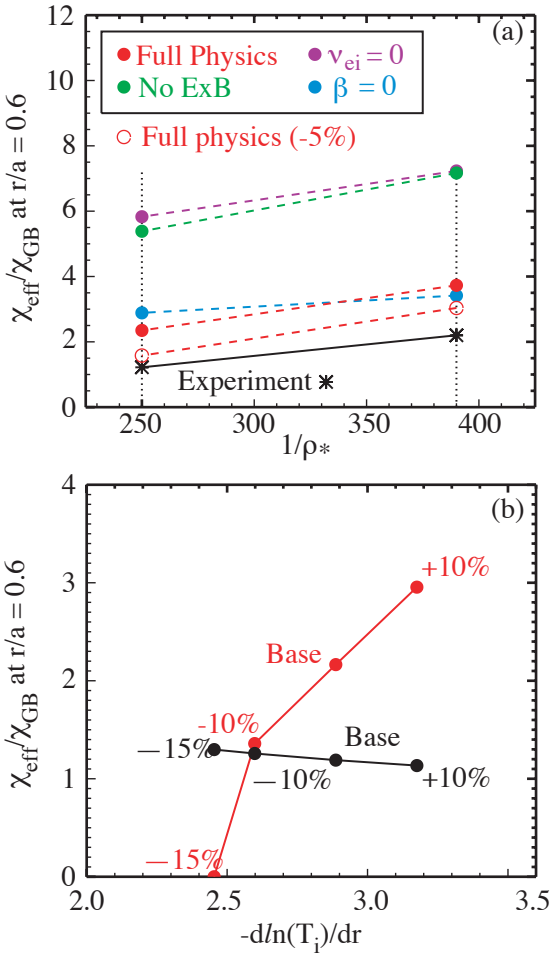

Fig. 2. Effective one channel energy diffusivity normed to gyroBohm at the r/a=0.6 norm point versus ρ_* comparing "full physics" for $\sqrt{m_i/m_e}$=60 with experiment and turning off ExB shear, electron-ion collisions, and finite beta in (a). Reductions in the in the ion temperature gradient from the base experimental values shown in (b) for the $\rho_* = 0.004$ case. A 5% reduction is shown in (a).

Bohm scaling ratio is lost and the gyroBohm scaled flux tube level of $\chi_{eff}/\chi_{GB} \approx 8$ is nearly obtained at the smaller ρ_*. [Curiously the best DIII-D H-mode pairs have significantly less ExB shear at r/a=0.6 which may account for their gyroBohm scaling (even with 1.5 times *larger* ρ_*).] Similarly electron-ion collisions de-trap the trapped electrons which increase the drive for the ITG turbulence; removing the collisions results in 2 times higher transport levels and a similar loss of the Bohm scaling. Finite beta, well below the ideal limit, typically weakens the transport somewhat. Here it weakens the tendency to Bohm scaling. All of these effects are in agreement with previous ITG-adiabatic electrons simulation with realistic profiles: specifically, that Bohm scaling is easier to obtain when the maximum growth rate is weakened with respect to the ExB shear rate [4]. In fact the core DIII-D L-mode transport is "stiff" and close to marginal transport. Figure 2(b) shows that even 10% reductions in the ion temperature gradient drive (well within experimental uncertainty), will allow the simulated and experimental power flows to match. This strongly suggests that the only way to verify agreement between theoretical models (or simulations) and experiments is by comparison of simulated and experimental temperature profiles with a gyrokinetic transport code.

We note in passing that the Kelvin-Helmholtz drive from the shear in the ion parallel velocity is quite modest for these discharges; the ion viscosity χ_ϕ is comparable to the ion energy diffusivity χ_i [$\chi_\phi/\chi_i = 0.85$ in the 5% reduction $\rho_* = 0.004$ case Fig. 2(a).] Only ExB transport has been shown; magnetic flutter transport is well below 10% of the electron energy transport at these β values (It is about 2% here although we have seen as high as 30% at 60% of the beta limit.) The DIII-D core has negligible convection and sits at a null flow

point with density gradient driven outflow in balance with an electron temperature gradient pinch flow.

The mechanism breaking the gyroBohm scaling is not entirely clear. Our previous circular ITG adiabatic electron simulations with realistic profiles in this range of DIII-D ρ_* values [4], clearly showed that gyroBohm scaling could be broken down to Bohm or worse when the purely diamagnetic local mode phase velocity shear rates $\gamma_s = (r/q)\partial(q/r)V_{mode}/\partial r \propto \rho_*[c_s/a]$ become comparable to local maximum growth rates [13]. The total mode phase velocity $V_{mode} = V_{mode\_0} + V_E$ has an intrinsic diamagnetic velocity and an ExB Doppler rotation velocity with is only partly diamagnetic. For the more realistic DIII-D simulations in Figs. 1 and 2, the ExB velocity shear results mostly from toroidal rotation. In fact the ExB shear rate (peaking near r/a=0.6 and passing through 0 at r/a=0.7 and near r/a=0.2-0.3) is virtually the same in both discharges and only slightly larger for the smaller ρ_* discharge. The diamagnetic component from the intrinsic mode velocity $\gamma_* = (r/q)\partial(q/r)V_{mode\_0}/\partial r$ is approximately 0.021 and 0.009 $[c_s/a]$ for $\rho_* = 0.004$ and 0.0026 respectively. These rates are just too small and actually oppose the ExB shear rate for co-injection toroidal rotation. (Curiously, it has been recently reported that counter-injected DIII-D H-modes have been found to have Bohm scaling whereas the normal co-injected H-modes has gyroBohm scaling [14]). The profile of γ_{max} is parabolic increasing from 0 at r/a=0.3 (i.e. a typical stable central core) to $0.3[c_s/a]$ at r/a/=0.6 and $0.37[c_s/a]$ at r/a=0.8. The γ_{max} profile is almost identical for the two discharges with the $\rho_* = 0.0026$ discharge very slightly lower (and not in the direction to cause Bohm scaling). This analysis does not favor the local velocity shear rate versus growth rate theory [13], and we turn to a possible nonlocal mechanism.

4. Nonlocal Effects Breaking GyroBohm Scaling

Our previous circular ITG adiabatic electron simulations with realistic but weakly sheared profiles showed that at weak driving, the turbulence appeared to drain from the unstable outer region and spread into the core {Fig. 4(b) of Ref. [4]}. χ/χ_{GB} decreased in the unstable region and increased in the stable region as ρ_* increased from 0.0025 to 0.0075. The spreading gave a super-gyroBohm scaling in the stable core, but a small breaking of gyroBohm toward Bohm in the unstable outer region. This effect is too weak for the small DIII-D ρ_* values to account for Bohm scaling. We believe this nonlocal turbulence spreading effect explains why turbulent transport results in an often stable central core when local transport models like GLF23 [15] suggest it should be quenched. In contrast, Lin et al. [16] and Hahm et al. [17] suggest that nonlocality is the key mechanism for Bohm scaling. They studied this "turbulence spreading" effect in circular ITG adiabatic electron global (GTC code) simulations with nearly a flat core profile ($0.3 < r/a < 0.7$) draining to a stable central core *and a stable edge*. The well studied "cyclone base" [18] parameters (typical of DIII-D) were set at r/a=0.5. These highly unphysical profiles did produce Bohm scaling for $0.004 < \rho_* < 0.008$ as later verified by GYRO [19].

We have recently re-examined [20] this nonlocal breaking of gyroBohm scaling to better quantify and understand its potential as a Bohm-scaling mechanism. We also suggest a heuristic theory to describe such nonlocal effects. Figure 3 shows GYRO ITG-adiabatic electron simulations with piecewise flat profiles with the r/a=0.6 DIII-D parameters from Figs. 1 and 2 (close to cyclone base parameters). There is no ExB shear or any kind of profile shearing; there is no variation in any term of the gyrokinetic equation except a sharp 4-fold drop in the driving ion temperature gradient at the left quarter of the radial slice providing a stable region. Runs with and without this stable region are shown. The maximum growth rates are γ_{max} = 0.167. 0.126, and 0.082 $[c_s/a]$ corresponding to the 0%, 15% and 30% reductions in the ion temperature gradient shown in Fig. 3. (These are two mode runs with $k_\theta\rho_s = (nq/r)\rho_s = [0, 0.3]$. Spot checks at the extremes with eight mode runs to $k_\theta\rho_s \le 0.7$ are entirely similar with perhaps 20% higher transport levels.) The runs without a stable core

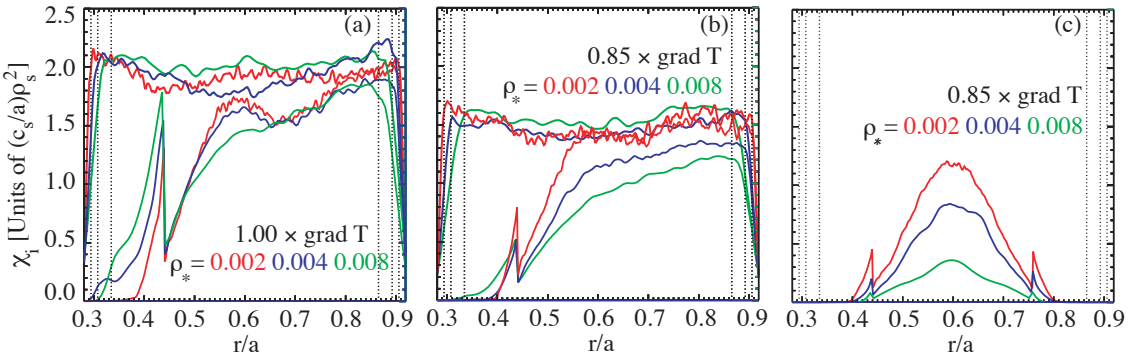

Fig. 3. Ion diffusivity normed to gyroBohm versus radius for ITG adiabatic electron piecewise flat profiles with DIII-D r/a=0.6 parameters from Figs. 1 and 2 in (a); ion temperature lowered by 0.85 in (b) and (c). Both left and right regions are stable in (c).

to the left show the gyroBohm scaling (χ/χ_{GB} independent of ρ_*). They have the same transport levels as flux tube runs with cyclic boundaries and prove that the zero value boundaries are benign. The runs with the stable core to the left show a tendency toward Bohm scaling to the outside and super-gyroBohm in the stable core. (The 4:1 sharp discontinuity in diffusivity is from our piecewise flat profile and reflects the definition of energy flux divided by temperature gradient; the energy flux is continuous.) Note that the "local hypothesis" [19] is satisfied: at every point the local diffusivity approached the local gyroBohm scaled diffusion as ρ_* gets sufficiently small. There is clearly a "nonlocality length" L proportional to the relative ion gyrolength and inversely to the maximum growth rate. This makes Bohm scaling more likely at smaller maximum growth rate. This is consistent with Fig. 2(a) and all our previous work (e.g. Ref. [4]). Figure 3(c) has a stable core to the left and an unphysical stable edge to the right. Clearly two sided drainage to both left and right greatly increases the nonlocal effect giving Bohm scaling for $0.004 < \rho_* < 0.008$ (as found in the case studied in Refs. [16,17,19].) We have checked that the adaptive source maintains the original driving temperature gradients.

A heuristic model can be made for incorporating gyroBohm breaking nonlocality into gyroBohm "local" transport models like GLF23 [15]: Such models use quasi-linear theory for the flows with a gyroBohm scaled spectral weight $I_k(x) = [(e|\tilde{\phi}_k|/T)/\rho_*]^2 \propto \gamma^{net}_{loc\_k}(x)/[c_s/a]$ where x is the local radius, and $\gamma^{net}_{loc\_k}$ the local linear ballooning mode growth rate for each mode k less the ExB shear rate. We propose to replace the local rate with a nonlocal rate

$$\gamma^{net}_k(x) = \int_{-\infty}^{\infty} dx'/[2L(x')]\gamma^{net}_{loc\_k}(x')\exp[-|x-x'|/L(x')] \quad .$$

It is easy to show [20] that for $x' < x_L$ ($x' > x_R$) the appropriate left (right) boundary condition is $\gamma^{net}_{loc\_k}(x') = \gamma^{net}_{loc\_k}(x_L)$ $\left[\gamma^{net}_{loc\_k}(x') = \gamma^{net}_{loc\_k}(x_R)\right]$ respectively. In the example of Fig. 3, if x_0 is the quarter box separation between the piecewise flat profiles, we can write $\gamma^{net}(x) = \gamma^{unstable}_{loc} f(x-x_0) - \gamma^{damped}_{loc} f(x_0-x)$ with $f(x-x_0) = [\Theta(x-x_0) - (1/2)Sign(x-x_0)\exp(-|x-x_0|/L)]$. $L(x')$ is again the nonlocal length which is taken to be a constant L here. As shown in Ref. [20] this model gives a good description of the nonlocal draining, a spreading effect shown in Fig. 3 provided L has the correct properties. For $L/a \propto \rho_* \to 0$ clearly $\gamma^{net}_k(x) \to \gamma^{net}_{0k}(x)$ and local gyroBohm scaling is recovered. For $L/a \to \infty$, $\gamma^{net}_k(x) \to \gamma^{net}_{glob\_k}$ the global eigenmode rate which tends to be a radial average of the local eigenmode rates [13]. Neither the local rates nor the global rates have a dependence on ρ_*. Global eigenmodes can form in a torus only because adjacent singular surfaces (with given n) are coupled and correlated by the curvature drifts, however it takes a long time to couple all the singular surfaces in the plasma, the number of which increase like $1/\rho_*$. They will tend to be sheared apart by the n=0 radial modes (zonal flows) before they can

completely form. It can be argued [20], that $L/a \propto 1/[\tilde{\gamma}_E T_{glob}]$. Counting the number of singular surfaces in the plasma and their toroidal connection rate, the global formation time is $T_{glob} = [1/\rho_*]sR/c_s$. The zonal flow ExB shearing rate is $\tilde{\gamma}_E = k_x^2 c\tilde{\phi}_k/B$. Since the zonal flow potentials scale in proportion to the high-n transport potentials, and $k_x\rho_s \approx k_y\rho_s \approx 0.3$, we find $L/a \propto [(\rho_*/s)(a/R)]/[\gamma^{net}_{loc\_k}/(c_s/a)]^\beta$ with $\beta = 1/2$. Figure 3 appears to suggest that $\beta \approx 1$ would give a better description. Note this heuristic argument suggests that nonlocality and any tendency to Bohm scaling is a toroidal property. Clearly adding a second (and unphysical) stable region to the right will double the drainage and the tendency to Bohm scaling in the flat profile unstable region. Only a detailed nonlocal model as outlined here and fit to the simulations of Fig. 3, can determine if this nonlocal drainage affect can describe the realistic Bohm scaling in Figs. 1 and 2. Although one can see some nonlocal effects in Fig. 1 (spreading into the stable region r/a < 0.3), the rather small variation with radial slice (at r/a=0.6) suggests nonlocal drainage is not significant here.

5. Profile Corrugations, Dynamos and the Neoclassical Current-voltage Relation, and Interaction of Turbulence and Neoclassical Flows

The most unexpected qualitative discovery made with GYRO simulations is that the flux-surface and time averaged n=0 "equilibrium" gradient profiles of density, temperature, and potential are corrugated on the scale of a few ion gyrolengths. Figure 4(a) shows an example for the electron temperature gradient. The profile consist of the smooth experimental profile input [green in Fig. 4(a)] plus the n=0 "zonal flow" perturbation: $T_0(r) = T_{0\_exp}(r) + \tilde{T}_0(r)$. $\tilde{T}_0(r)/T_0(r) \approx O(\rho_*)$ is small but the basic saturation rule is $\partial\tilde{T}_0(r)/\partial r \approx \partial T_0(r)/\partial r$. The surprise is that while these perturbations do fluctuate and move around in radial position, they do not time average to zero over a few milliseconds. Instantaneous or shorter term averages will be perhaps twice as large but longer time averages show no decrease. The reason appears to be that the corrugations are tied to singular surfaces which do not move in time. As shown in Fig. 4, the corrugations line up on the lowest order rational surfaces in this 16-mode $\Delta n = 6$ simulation. The transport levels and corrugation size are the same for a 32-mode $\Delta n = 3$ simulation, except there will be a few more lower order surfaces. In fact the radial divergence of any flux surface average radial turbulent flow will show similar corrugations localized about singular surfaces. For example we have shown [21], that the radial divergence of the turbulent radial flow of parallel current gives a corrugated turbulent dynamo EMF and toroidal current density localized on singular surfaces: $-r^{-1}\partial r\Gamma_x^J/\partial r = (\omega_{pe}^2/4\pi)E_{dyn}$, $J_{dyn} = \sigma_{neo}E_{dyn}$, with $E_{dyn} = [T_e/ea]\rho_*^2\hat{E}_{dyn}$ for gyroBohm scaling. Figure 4(b) shows an example. The current density corrugations could easily be 150% of background in DIII-D $\left[J_{dyn}/J = \hat{E}_{dyn}/\hat{E}_A\right]$. In the massless electron limit, this magnetic flutter dynamo can be related to the MHD "alpha dynamo" [21]. A second electrostatic dynamo related to the electron parallel nonlinearity [22] [$\hat{E}^{II}_{dyn}$ in Fig. 4(b)] is smaller but less corrugated. Integrating over radius neither appears to drive significant total current and we expect little deviation from the neoclassical current-voltage relation. However the corrugations of current density could have a significant effect on Δ' determining tearing mode stability. The corrugations in temperature and density gradients will also cause corrugations in the bootstrap currents.

Radial transport flows result from three mechanisms: ExB fluctuations $\langle\tilde{v}_{Ex}\tilde{g}\rangle$, and magnetic flutter $\langle v_{||}\tilde{B}_x/B_0\tilde{g}\rangle$, as well neoclassical curvature drifts $\langle v_{dx}\tilde{g}\rangle$ ($\tilde{g}$ is the non-adiabatic fluctuation and/or deviation from the flux surface average Maxwellian distribution function $\langle\ \rangle$ denotes flux surface and time average.) The usual turbulent flows result from the beating of n > 0 fluctuations. The n=0 radial modes (or zonal flows) could contribute to the standard neoclassical flows which arise from flux surface deviations. It is easy to show that including only the cross field nonlinearity, there can be no interference or "cross talk" between turbulent and standard neoclassical flows at vanishing ρ_*; i.e. the flows are simply additive as generally assumed. We have recently shown [23] that this also holds to a good approximation for finite ρ_* in DIII-D. By adding the n=0 neoclassical driver and neoclassical flow diagnostic to GYRO, we have extended the (n=0 only) large orbit neoclassical gyrokinetic simulations by

Wang, Hinton, and Wong [24] to look for "cross talk". Figure 5 shows an ITG adiabatic electron simulation with no ExB shear with the n=0 neoclassical driver and conservative Krook model ion-ion collisions turned "on" and "off". Since the collisions slightly stabilize the n=0 radial modes the $n > 0$ transport is slightly higher. Otherwise the neoclassical driver has little if any significant effect here. The neoclassical driver ($\vec{v}_{dx}(\theta)\cdot[\vec{\nabla}F_0 - (e/T)\vec{\nabla}\Phi_0]$) contains the input ion temperature and density gradients as well as potential gradients and induces the neoclassical parallel ion velocity profile which (if strong enough) could drive Kelvin-Helmholtz via the nonlinear interaction with $n > 0$ modes. (When the neoclassical driver is neglected, the parallel velocity shear is added directly to ω_* terms). Figure 5(b) shows that the ion neoclassical energy diffusivity radially averaged over the corrugations close to the non-turbulent large-orbit [24] diffusivity. Clearly both ion-ion collisions and the neoclassical driver which induces n=0 perturbations to have $O(\rho_*)$ deviations from the flux surfaces are required to get significant neoclassical transport. Otherwise, the neoclassical flows in the corrugations will average out. The radial average neoclassical plasma flow is ambipolar and negligible. (Note again that the energy diffusivities are flows divided by temperature gradients. When the neoclassical diffusivity is added to the ExB, the total is positive.)

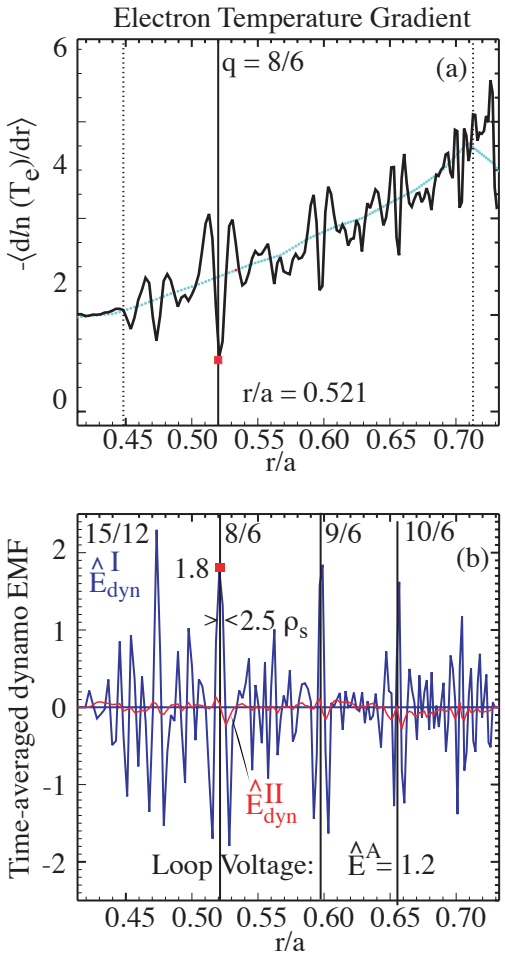

Fig. 4. Millisecond time average corrugations in the electron temperature(a) and dynamo current density (b) vs radius using DIII-D parameters of the $\rho_* = 0.004$ Figure 2(b) case with power flows matched to experiment. Low order singular surfaces are noted. The flow divergence magnetic flutter dynamo $\hat{E}^{I}_{dyn}$, the electrostatic parallel nonlinearity $\hat{E}^{II}_{dyn}$, and the DIII-D transformer EMF are indicated. ($\sqrt{m_i/m_e}$ =60.) $700 < tc_s/a < 1100$.

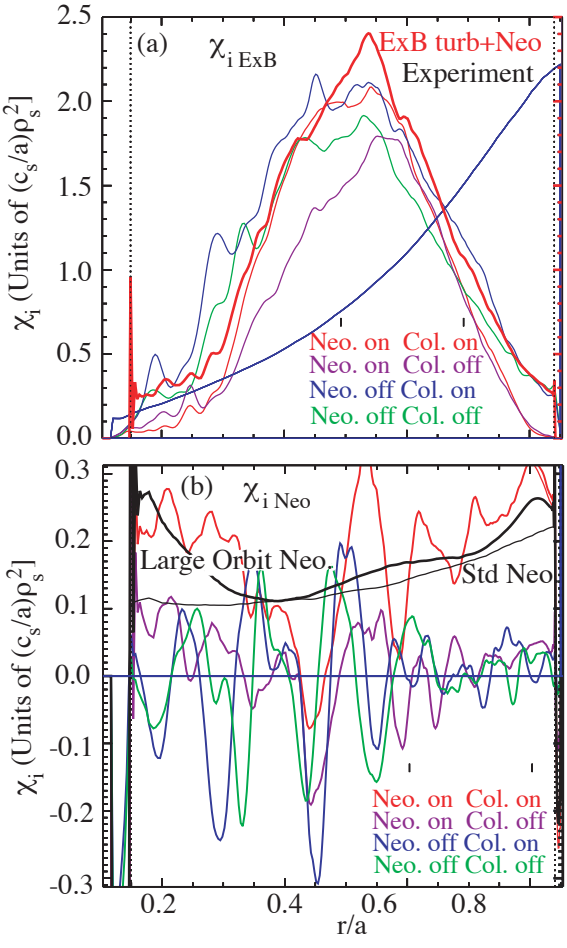

Fig. 5. Ion ITG-adiabatic electron ExB turbulent energy diffusion profile compared with experimental in (a) with neoclassical energy diffusivity profile in (b). DIII-D parameters of the $\rho_* = 0.004$ with ExB equilibrium shear stabilization turned off. Both large-orbit and standard vanishing ρ_* neoclassical are shown.

Acknowledgment

Work supported by U.S. Department of Energy under DE-FG03-95ER54309 and in part by the SciDAC Plasma Microturbulence Project. We are grateful to M.R. Fahey and the ORNL Center for Computational Science for special access to the CrayX1 256ps (Phoenix) and IBM Power4 (Cheetah) computers. This paper is dedicated to our teacher and colleague, the late Prof. M.N. Rosenbluth.

References

[1] CANDY, J., WALTZ, R.E., J. Comput. Phys. **186** (2003) 545.
[2] DORLAND, W.F.F., KOTSCHENREUTHER, M., ROGERS, B.N., Phys. Rev. Lett. **85** (2000) 5579.
[3] PARKER, S.E., CHEN, Y., WAN, W., COHEN, B.I., and NEVINS, W.M., Phys. Plasmas **11** (2004) 2594.
[4] WALTZ, R.E., CANDY, J., and ROSENBLUTH, M.N., Phys. Plasmas **9** (2002) 1938 (APS 2001).
[5] FREIMAN, E. A., and CHEN, L., Phys. Fluids **25**, 502 (1982); ANTONSEN, T.M., and LANE, B., ibid **23**, 1205 (1980).
[6] PARECHI, L., and RUSSO, G., in *Hyperbolic Problems: Theory, Numerics and Application,* (Proc. 9th Int. Conf. on Hyperbolic Problems, Pasadena, CA 2002) (Springer-Verlag, Heidelerg, 2003).
[7] MILLER, R.L., CHU, M.S., GREENE, J.M., LIU, Y.-R., and WALTZ, R.E., Phys. Plasma **5**, 973 (1998).
[8] WALTZ, R.E., and MILLER, R.L., Plasma **6**, 4265 (1999).
[9] WALTZ, R.E., DeBOO, J.C., and ROSENBLUTH, M.N., Phys. Rev. Lett. **65** (1990) 2390.
[10] CANDY, J., WALTZ, R.E., Phys. Rev. Lett. **91** (2003) 045001.
[11] McKEE, G.R., PETTY, C.C., WALTZ, R.E., et al., Proc. 18th IAEA Fusion Energy Conf., Sorrento, Italy, 2000) Paper EX6/5.
[12] WALTZ, R.E., KERBEL, G.D., and MILOVICH, J., Phys. Plasmas **1**, 2229 (1994); ibid. **2**, 2408 (1995) (APS 1994); WALTZ, R.E., DEWAR, R.L., GARBET, X., ibid **5** (1998) 1784 (APS 1997).
[13] GARBET, X., and WALTZ, R.E., Phys. Plasmas **3**, 1898 (1996) (APS 1995).
[14] PETTY, C.C., WADE, M.R., KINSEY, J.E., BAKER, D.R., and LUCE, T.C., Phys. Plasmas **9**, 128 (2002).
[15] WALTZ, R.E., STABLER, G.W., DORLAND, W., HAMMETT, G.W. ,KOTSCHENREUTHER, M., and KONINGS, J.A., Phys. Plasmas **4** (1997) 2482.
[16] LIN, Z., ETHIER, S., HAHM, T.S., and TANG, W., Phys. Rev. Lett. **88** (2002) 195004.
[17] HAHM. T.S., DIAMOND, P.H., LIN, Z., ITOH, K., ITOH, S.-I., Plasmas Phys. Control. Fusion **46** (2004) A323.
[18] DIMITS, A.M., BEER, M., et al., Phys. Plasmas **7** (1997) 969.
[19] CANDY, J., WALTZ, R.E., DORLAND, W., Phys. Plasmas **11** (2004) L25.
[20] WALTZ, R.E., and CANDY, J., "Heuristic theory of nonlocally broken gyroBohm scaling" to be submitted to Phys. Plasmas.
[21] HINTON, F.L., WALTZ, R.E., and CANDY, J., Phys. Plasmas **11** (2004) 2594 (APS 2003).
[22] ITOH, S.-I., and ITOH, K., Phys. Lett. A **127** (1988) 267.
[23] WALTZ, R.E., CANDY, J., and HINTON, F.L., "Gyrokinetic simulation of neoclassical flows embedded in turbulence" to be submitted to Phys. Plasmas.
[24] WANG, W., HINTON, F.L., and WONG, S.K., "Neoclassical radial electric field and transport with finite orbits," Phys. Rev. Lett. **87**, 055002-1 (2001).